SCIENTIFIC REPORTS

OPEN

SUBJECT AREAS:
CLIMATE-CHANGE IMPACTS
GEOMORPHOLOGY

Received
26 February 2014

Accepted
18 July 2014

Published
15 August 2014

Correspondence and requests for materials should be addressed to G.A. (alexandrakis@iacm.forth.gr)

# An holistic approach to beach erosion vulnerability assessment

George Alexandrakis[1] & Serafim E. Poulos[2]

[1]Institute of Applied and Computational Mathematics, Foundation of Research and Technology, Hellas, [2]Faculty of Geology & Geoenvironment, Department of Geography & Climatology, University of Athens, Athens, Greece.

**Erosion is a major threat for coasts worldwide, beaches in particular, which constitute one of the most valuable coastal landforms. Vulnerability assessments related to beach erosion may contribute to planning measures to counteract erosion by identifying, quantifying and ranking vulnerability. Herein, we present a new index, the Beach Vulnerability Index (BVI), which combines simplicity in calculations, easily obtainable data and low processing capacity. This approach provides results not only for different beaches, but also for different sectors of the same beach and enables the identification of the relative significance of the processes involved. It functions through the numerical approximation of indicators that correspond to the mechanisms related to the processes that control beach evolution, such as sediment availability, wave climate, beach morhodynamics and sea level change. The BVI is also intended to be used as a managerial tool for beach sustainability, including resilience to climate change impact on beach erosion.**

Beaches are by nature unstable coastal landforms as they respond to changes in sediment supply, nearshore hydrodynamics and sea level. Across Europe, coastal erosion has been a longstanding, large-scale issue[1] with more than 40% of the beaches in France, Italy and Spain being under erosion[2]. Similarly, in the USA[3] of the 33,000 km of eroding shoreline, some 4,300 km are beaches[3]. Moreover, beach erosion poses a major threat not only to interconnected ecosystems[4], but also to stakeholders, as it is related to beach property values[5] and tourism[6].

Beach evolution depends on processes such as sediment availability[7], storms causing changes that persist with time[8], complex interactions between nearshore and onshore sedimentary bodies[9], sea level rise[10,11] and the broader coastal geological setting[12]. Erosion, on the other hand, is usually the combined result of a wide range of factors, both natural (e.g. winds, storms, nearshore currents) and human-induced (e.g. coastal engineering, river basin regulation) that operate on different time and spatial scales[13].

Thus, quantification of these factors becomes more difficult due to their variability and coupling of the processes that affect coastal areas, and also to the frequency at which coastal changes occur[14]. The estimation of the vulnerability of coastal areas to erosion has received considerable attention and a vast literature is available in this field; however, most of this is associated with sea level rise, induced by climate change[15–18]. In the case of beaches, early attempts were based upon simple approaches[19–21], focusing on erosion due to sea level rise. More recently, methods estimating vulnerability associated with storms have been developed[22–26].

To this direction, we present an index dedicated to the assessment of vulnerability to erosion exclusively of beaches, considering the predominant hydro- and sediment- dynamic processes that contribute to beach evolution. Moreover, the new Beach Vulnerability Index (BVI) refers to beaches, regardless their size, and to the features of the associated coastal environments, incorporating processes operating over long (e.g. a gradual change in sea level) and short (i.e. storm events) time periods. Special effort has been placed upon the index estimation in order to require easily obtainable data and to avoid calculations demanding high processing capacity.

## Index Development

The idea of the Beach Vulnerability Index (BVI) originates from the Coastal Vulnerability Index developed by Gornitz et. al.[15]. It is based on a numerical approximation of the principal physical processes that control the evolution of a beach; these, in turn, are related to sediment availability (terrestrial, aeolian and marine), nearshore hydro- and sediment- dynamics and relative sea level change[27]. Subsequently, we have identified the following mechanisms to consider as indicators that are related to the aforementioned processes: (i) long-shore sediment transport; (ii) cross-shore sediment transport; (iii) riverine sediment inputs; (iv) the effect of sea level change; (v)

erosion of associated coastal landforms; (vi) wave run up; and, (vii) aeolian transport. The calculation of these mechanisms incorporates a large number of parameters related to nearshore hydrodynamics (e.g. wave breaking characteristics, energy flux within the nearshore zone), sediment dynamics (e.g. threshold of sediment movement, beach morphodynamic characteristics), aeolian transport of beach material (e.g. wind speed and direction, beach grain size) and the terrestrial supply of sediment (e.g. riverine sediment influx, advection of erosion products from neighbouring coastal landforms). For the numerical estimation of the above mechanisms existing data-sets (e.g. wind/wave climate), simple *in-situ* measurements (e.g. beach profiling), grain-size analysis and common numerical modelling (e.g. wave refraction, wave breaking characteristics) could be utilised. Thus, the BVI expands its applicability as its estimation does not need massive or difficult to be collected, data or demanding computing capacity.

The B.V. Index calculation follows a four step procedure: (1) identification of beach physiographic, climatic and oceanographic characteristics; (2) division of the beach in characteristic sectors, according to step 1; (3) calculation of vulnerability indicators; and, (4) index estimation (figure 1).

The first step includes the identification of geomorphological and oceanographical characteristics of the beach, together with climatic conditions of its hinterland. The geomorphological characteristics refer to nearshore bathymetry, beach slope, width and granulometry. Beach profile characteristics (slope, profile length) are estimated by taking into account tidal range[28], while the oceanographic characteristics refer to incoming waves (significant height, period and length, closure depth) and those at wave breaking (height, angle and depth). Climatic conditions are considered also for aeolian transport (wind speed and direction). In the case of riverine influxes, the climatic (air-temperature, precipitation) and hydrological characteristics of the catchment area are included. For the parameterisation of the aforementioned characteristics that control sediment availability, four categories of data are required (figure 1), i.e. morphological, sedimentological, climatic and hydrodynamic.

In the second step, the beach is divided into alongshore sectors, with width that is dependent upon the required resolution in each case study and on the basis that each sector is homogenous in terms of geomorphological (e.g. the presence of a river mouth or dune field), sedimentological (different granulometry) and wave climate characteristics (e.g. due to varying shoreline orientation). In the calculations, each sector is represented by a profile aligned normally to the shoreline, with mean tidal elevation defining shoreline position. The landward upper limit of the beach profile may be either a morphological change (e.g. the base of a coastal cliff, or a dune), or a human construction (e.g. coastal wall). In order to define the seaward limit of each sector, the approach of defining the closure depth is adopted; the latter is calculated using the Hallermeier[29] formula, which basically depends on the storm wave characteristics that are considered to be associated with the maximum observed waves.

$$h_c = 2.28H_e - 68.5\left(\frac{H_e^2}{gT_e^2}\right) \quad (1)$$

where, g is the acceleration of gravity (m/s$^2$), $H_e$ is the storm wave height before breaking (m), and $T_e$ is the corresponding wave period.

The third step addresses the calculation of the seven (7) indicators (mechanisms) that correspond to the aforementioned processes and are used for the estimation of the index. Each indicator is defined probabilistically by using the weighted average value with respect to the frequency of occurrence for a 30-year period. This is similar to the way that Bosom and Jiménez[23] estimate the probabilistic vulnerability of beaches to storm events. Each indicator is characterised as positive if it indicates sediment loss and negative if it involves sediment gain. The homogenisation of all indicators is achieved by converting them into non-dimensional values, dividing their average value with their maximum values and expressing the ratios produced as percentages.

## Indicators

The calculation of the seven indicators is based on the application of mathematical relationships, which have been selected after several tests considering their acceptability, reliability, simplicity, and data demand.

The **Long-shore sediment transport** ($Q_l$) indicator is estimated by the ratio:

$$Q_l = 100\frac{Q_{l\,WHA}}{Q_{l\,max}} \quad (2)$$

where, $Q_{l\,max}$ is considered to be the potential volumetric longshore transport rate and $Q_{l\,WHA}$ corresponds to the weighted average value with respect to the frequency of wave occurrence; the latter is justified by the wave heights that currents with velocities exceeding the threshold for sediment movement[30] can produce:

$$U_{wle} = 2\pi C\left[1+5\left(\frac{T_r}{T_o}\right)^2\right]^{-1/4} \quad (3)$$

where, To is the period of the incoming offshore waves, while C and $T_r$ are coefficients deriving from $s_*$, a scaled dimensionless immersed sediment weight, provided by the following relationships:

$$C = \frac{2.53vs_*^{0.92}}{4D_{50}} \quad (4)$$

$$T_r = \frac{159s_*^{-1.3}D_{50}}{v} \quad (5)$$

$$S_* = \frac{D_{50}\sqrt{P_S g D_{50}}}{4v} \quad (6)$$

where, $U_{wle}$ is critical boundary velocity (m/s); $T_o$ is wave period (m), $D_{50}$ is grain size (mm); v is kinematic viscosity of seawater ($\sim 1{\cdot}10^{-6}$ m$^2$/sec); and $\rho_s$ is sediment density (gr/cm$^3$).

To estimate the $Q_{l\,WHA}$ and $Q_{l\,max}$ values, the Komar[31] formula has been used, since it provides a very good estimation for longshore sediment transport, with the only requirement being that of wave breaking characteristics:

$$Q_l = 1.1\,\rho g^{3/2}H_b^{5/2}\sin a_b \cos a_b \quad (7)$$

where, $Q_l$ is potential volumetric longshore transport rate (m$^3$/day), ρ is water density (gr/cm$^3$), g is acceleration of gravity (m/sec$^2$), $H_b$ is breaking wave height (m), and $a_b$ is wave breaking angle.

The **Cross-shore sediment transport** ($Q_C$) indicator is given by the ratios:

$$Q_c = \begin{cases} 100\dfrac{Q_{c\,WHA}}{Q_{c\,max}}\,(\text{offshore}) \\ 100\left(1-\dfrac{Q_{c\,WHA}}{Q_{c\,max}}\right)(\text{onshore}) \end{cases} \quad (8)$$

where, $Q_{c\,max}$ is potential volumetric cross-shore transport rate, and $Q_{c\,WHA}$ is the cross-shore sediment transport for those wave heights that exceed the corresponding threshold of the critical boundary velocity ($U_{wle}$), in respect to the frequency of occurrence. The direction of sediment movement is estimated by the use of the criterion[32], given by the following relationship, while offshore values are regarded as positive, and onshore values as negative.

$$\frac{gH_o\tan\beta T}{L_o w_s}\begin{cases} >0.5(offshore) \\ <0.5(onshore) \end{cases} \quad (9)$$

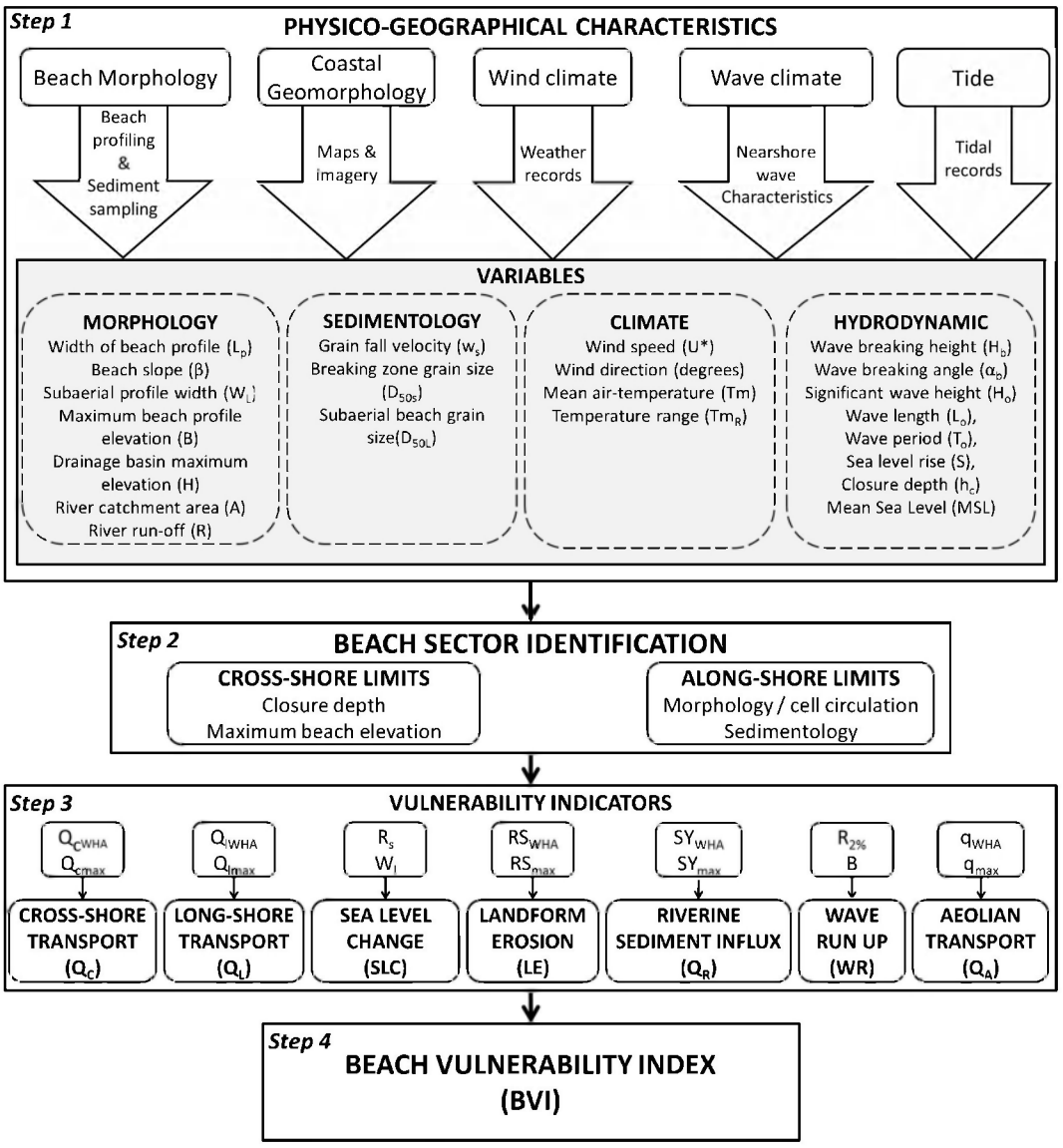


**Figure 1** | **Flow chart of the calculation method for the Beach Vulnerability Index.**

The values for the indicator expressing the cross-shore sediment transport ($Q_c$) are calculated with the use of the equation[33]:

$$Q_c = pC_D u_m^3 \left\{ \frac{B}{\tan\varphi} \left( \psi_1 + \frac{2}{3}\delta_u - \frac{\tan\beta}{\tan\varphi} u_5^* \right) + \frac{u_m}{w_S} \left[ \psi_2 + \delta_u u_3^* - \frac{u_m}{w_S} \varepsilon_S u_5^* \tan\beta \right] \right\} \quad (10)$$

where, $\varepsilon_B = 0.2$; $\varepsilon_S = 0.025$; $C_D$ = drag coefficient; $w_s$ = sediment fall velocity (m/s); $\varphi$ = the angle of repose; $\beta$ = the beach slope; $u_b$ = near bed water velocity (m/s); $\rho$ = water density (gr/cm$^3$); and, $\rho_s$ = density of sediment (g/cm$^3$); $\delta_u$, $\psi_1$, $\psi_2$, $u_m$, $u_3$*, and $u_5$* = cross-shore velocities (m/s).

The cross-shore ($\delta_u$, $\psi_1$, $\psi_2$, $\psi_1$, $u_3$* and $u_5$*) variables expressed as a function of significant wave height are given by the relationships[34]:

$$\psi_1 = 0.303 - 0.00144\ H_o \quad (11)$$

$$\psi_2 = 0.603 - 0.00510\ H_o \quad (12)$$

$$\delta_u = 0.458 - 0.00157\ H_o \quad (13)$$

$$u_m = 31.9 + 0.403\ H_o \quad (14)$$

$$u_3^* = 0.548 + 0.000733\ H_o \quad (15)$$

$$u_5^* = 1.5 + 0.00346\ H_o \quad (16)$$

The Bailard and Inman formula[33] was used because it is the only one that does not require detailed field data and it can provide satisfactory results[33].

The **Riverine sediment influx** ($Q_R$) indicator is given by the ratio:

$$Q_R = 100\left(1 - \frac{SY_{WHA}}{SY_{max}}\right) \quad (17)$$

where, the values $SY_{WHA}$ and $SY_{max}$ correspond to weighted average values, for a 30-year period, in respect to the frequency of occurrence and maximum freshwater discharge values respectively. $Q_R$ receives a negative sign in calculations, as it corresponds to sediment gain. For the estimation of river sediment flux, the Hovius formula[35] is used:

$$\ln SY = -0.416 \ln A + 4.26\cdot10^{-4}H + 0.15H + 0.15T_m + 0.095T_{mR} + 0.0015R + 3.58 \quad (18)$$

where, A is the catchment area ($m^2$), H is the maximum elevation of the drainage basin (m), $T_m$ is the mean temperature (°C), $T_{mR}$ is temperature range (°C), and, R is river run-off ($m^3/s$) (all attributes are treated as dimensionless).

In cases where there is no sediment supply from riverine systems, the indicator reaches its maximum value (i.e. 100). This method of estimating riverine sediment influx, although does not take into consideration sediment availability in the catchment area, was depicted after it was tested with similar formulae[36,37] and was found to produce good results[38]. In addition, it satisfies the criterion of broad applicability, as all the incorporated attributes related to the catchment area are easily acquired.

The **Coastal Landform Erosion (LE)** indicator expresses the contribution of coastal landform erosion in the displacement of the shoreline. It is given by the ratio:

$$LE = 100\left(1 - \frac{RS_{WHA}}{RS_{max}}\right) \quad (19)$$

where, RS is the difference between the present ($R_1$) and future ($R_2$) shoreline position, $RS_{WHA}$ and $RS_{max}$ corresponds to the weighted average value in respect to the frequency occurrence of the prevailing wave and storm wave conditions, respectively. For the calculation of the RS, the following formula[39] is used:

$$RS = R_2 - R_1 = \frac{(S_2 - S_1)L_p}{p(B + h_c)} \quad (20)$$

where, $S_1$ και $S_2$, expressed in metres, correspond to historical and expected sea level rise, respectively, $L_p$ is the profile length (m), **B** is berm height (m), P is the proportion of coarse sediment that is adequate to retain the shore profile in equilibrium, and $h_c$ is closure depth (m).

The selection of this formula is based on the comparison of its estimates to the results of other more detailed calculations, such as that provided by the SCAPE model[40].

The **Sea Level Change (SLC)** indicator is given by the relationship:

$$SLC = 100\left(\frac{R_S}{W_1}\right) \quad (21)$$

where, $R_s$ corresponds to the weighted average conditions in respect to frequency occurrence and $W_1$ is the beach width.

The shoreline retreat due to relative sea level change is given by the Dean semi-empirical relationship[20], which produces better results than others[41], by incorporating storm surge and wave set-up variables:

$$R_S = (S + 0.068H_b)\frac{W}{d_b + B} \quad (22)$$

where, **B** is berm height (m), $H_b$: is wave breaking height (m), S is relative sea level rise (m), W is profile length (m), and $d_b$ is breaking depth (m).

The selected equation 22 presents certain deficiencies, as it originates from the Brunn rule[42] that has been extensively criticised, due to the assumptions involved and because it omits many important variables[43]. On the other hand, it seems to provide satisfactory results, when compared to other static or dynamic approaches[44]. Therefore, it is considered adequate to quantify this indicator, keeping in mind that variables which control erosion rates are addressed in the index by other indicators.

**The Wave Run-up (WR)** indicator is provided by the ratio:

$$WR = 100\left(\frac{R_{2\%}}{B}\right) \quad (23)$$

where, $R_{2\%}$ is wave run-up for the 2% of maximum incoming waves, whilst the maximum beach elevation (B) is considered as maximum value.

The estimation of $R_{2\%}$ has been made with the use of the Stockton's et. al., formula[45], since it has been proved in other cases, that it provides better results than other approaches on the basis of field measurements and coastal imaging analysis[46].

$$R_{2\%} = 1.1\left(0.35\,\beta\sqrt{\frac{H_o}{L_o}} + \frac{\left[H_oL_o(0.563\,\beta^2 + 0.004)\right]^{1/2}}{2}\right) \text{ (all beaches)} \quad (24)$$

$$R_{2\%} = 0.043\sqrt{H_oL_o} \text{ (dissipative beaches)} \quad (25)$$

where, $H_o$ is offshore significant wave height (m); Lo is offshore wave length (m), and β is beach slope (in rads).

The **indicator related to aeolian transport ($Q_A$)** with respect to the direction of movement is given by the ratios:

$$Q_A = \begin{cases} 100\dfrac{q_{WHA}}{q_{max}} \text{ (seawards)} \\ 100\left(1 - \dfrac{q_{WHA}}{q_{max}}\right) \text{ (landwards)} \end{cases} \quad (26)$$

The aeolian transport rate q (in $gm/cm^2/s$) is estimated using the Hsu empirical formula[47], since it has proved to have very good correlation with field measurements[48].

$$q = V_aP_a\left(e^{-0.63 + 0.91D_{50L}}\right)\left[\sqrt{\frac{U^*}{gD_{50}}}\right] \quad (27)$$

where, U* is shear velocity (m/s), g is acceleration of gravity ($m^2/s$), $D_{50}$ is mean grain size (mm), Va is air kinematic viscosity ($m^2/s$), and $\rho_a$ is mass air density ($g/cm^3$).

The mean ($q_{WHA}$) transport rates correspond to the weighted average conditions with respect to wind frequency of occurrence, while the maximum ($q_{max}$) rates correspond to maximum values of shear velocity (U*). The threshold for the aeolian sediment transport is provided by the formula[49]:

$$U_{ut} = A_t\sqrt{\frac{(p_s - p_a)gD_{50}}{p_a}} \quad (28)$$

where, $U_{ut}$ is critical boundary air velocity (m/s), $A_t$ is a dimensionless coefficient equal to 0.118, and $\rho_s$ is mass density of the sediment ($g/cm^3$).

## Index calculation

We have calculated Beach Vulnerability Index (BVI) as being the arithmetic mean of the above mentioned vulnerability indicators:

$$BVI = \frac{Q_1 + Q_c + LE + Q_A + WR + SLC + Q_R}{7} \quad (29)$$

The arithmetic mean was chosen after several tests were conducted with other types of statistical mean (e.g. geometric mean, root mean square) and after considering the different approaches adopted in the calculation of other indices. Therefore, this approach, considering all indicators of equal importance, reduces, not only subjectivity[50], but it also permits identification of the relative significance of index indicators.

Subsequently, the index values are expressed as percentages (0-100%) and ranked into five classes, following the application of normal distribution to the total number of beach sectors involved in the analysis. The five statistical classes produced, on the basis of the mean value (μ) and standard deviation (σ), correspond to the five categories of beach vulnerability (figure 2): very low (1); low (2); medium (3); high (4) and very high (5).

**Data requirements.** The data needed for the calculation of index indicators could be distinguished in two main categories: (i) raw data, deriving from maps (e.g. topographic), aerial photographs

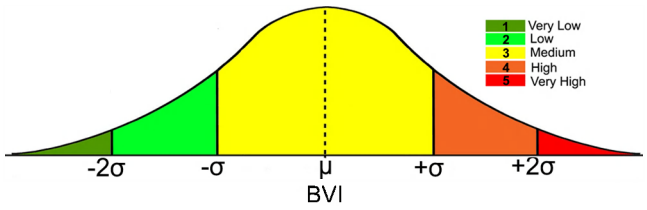


**Figure 2** | The five (5) categories of Beach Vulnerability Index (μ is the geometric mean; and σ is the standard deviation).

and satellite images, obtained by field observations and measurements (e.g., shore normal profiles) and laboratory analyses (e.g., grain size); and (ii) analytical data, produced by analysing the above mentioned raw data as well as those gathered from literature search (e.g. wind data). In figure 1, the required data for the BVI application is presented analytically. As aforementioned, the calculation of index indicators has aimed to satisfy both data availability and low economic resource for obtaining the required data, while their analyses aspire to be accomplished using reasonable computing efforts (see also Methods section). Moreover, it is worth mentioning that some countries have started to develop databases with the required data sets (e.g. the U.K.[51]).

## Index testing

We have applied the Beach Vulnerability Index to 18 beaches, divided in 138 beach sectors, around the Greek coastline (Figure 3a) that are characterised by different physio-geographical characteristics, in terms of associated coastal landforms (sand dunes, deltas, lagoons, coastal cliffs), incoming wave regime (open coast, semi-protected), geological setting and beach material (i.e., grain size). The mean values of the seven indicators, together with the overall classification of their vulnerability, are presented in table 1, while a graphical output for the beach of Agia Anna (location 14) is presented in figure 3b. In the case of Agia Anna beach (figure 3b) the index indicators are associated with significantly different values over the nine (9) beach sectors. Thus, the mean longshore transport indicator ($Q_l$) is estimated to be 15.08, but it is associated with zero value in Sectors 2, 6 and 7; Sector 3 presents the maximum estimated value (29.30). For the cross-shore ($Q_c$) indicator, the mean value is 41.62, varying from 31.64 (Sector 1) to 46.77 (Sector 3). Wave run-up (WR) values range from 13.45 (Sector 7) to 64.88 (Sector 9), with the mean value being 26.92. The Aeolian transport ($Q_A$) indicator has a mean value of 8.73, being zero in all sectors except in Sectors 3 (38.21) and 4 (40.35). The sea level change indicator (SLC) gives values, which vary from 2.24 (Sector 3) to 9.61 (Sector 1), whilst its mean value is 3.43. The riverine inputs indicator ($Q_R$) has a maximum value (100) in Sectors 1–4, as these sectors do not receive the river Boudouros influxes. In Sectors 5 and 6, $Q_R$ presents values 57.59 and 56.70, respectively, while in the northern Sectors 7 to 9 it is characterised with very low values (<4). The land erosion indicator (LE) has a minimum value in Sector 3 (35.12) and a maximum value in Sector 9 (72.49), while the mean value of 58.69. Finally, BVI values vary from 19.51 (Sector 1) to 37.97 (Sector 4), having a mean value of 30.09. On the basis of the statistical analysis for the 138 sectors of the 18 beaches included in the analysis, the values justifying the 5 categories of vulnerability, on the basis of their median (33.96) and standard deviation (11.38) are: very low (<11); low (11–22); medium (34–45); high 34–45; very high (>45). Hence, Sectors 1, 2 and 5–9 are subjected to moderate vulnerability (29.0–38.8), whilst Sectors 3 and 4 to are subjected to low vulnerability (19.2–29.0).

In most of the study areas the riverine influx indicator attains its maximum value (100), indicating high vulnerability. This is due to the fact that most of the beaches involved in this analysis do not host active river mouths, while in a few cases either sediment influx is retained behind dams or river mouths have been subjected to artificial regulation (e.g. offshore channel prolongation).

**Index results and beach behavior patterns.** The results of the BVI were found to be in very good correlation with the behaviour patterns of the beaches involved in the analysis. Characteristically, we refer to three beaches with different physico-geographical characteristics (figure 4). In the case of Almiros beach (location 2, figure 3), vulnerability values are increasing from west to east, suggesting higher erosion rates eastwards; this is in agreement with the observations that the the eastern and central part of the Almiros bay have retreated up to 15 m during the past 25 years, while its western part seems to be rather stable[52]. In the case of Ammoudara

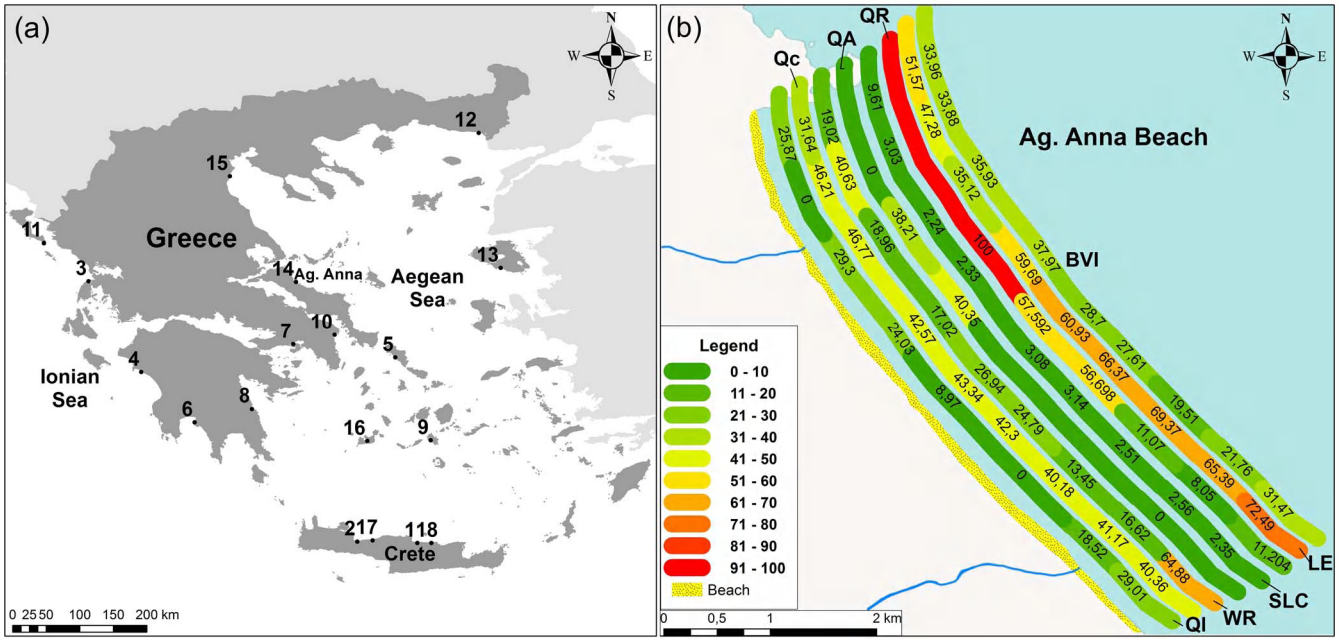


**Figure 3** | The locations of the case study areas mentioned in table 1 (a); and graphical presentation of BVI application in the case of the Ag. Anna beach (b). Maps were created with ArcMap 9.3.

Table 1 | Mean values of the indicators used in the BVI calculation, together with their vulnerability ranking

| Beach | | No Sectors | $Q_L$ | $Q_c$ | WR | $Q_A$ | SLC | $Q_R$ | LE | BVI | Rank |
|---|---|---|---|---|---|---|---|---|---|---|---|
| **1** | **Ammoudara** | 13 | 4.44 | 11.30 | 13.81 | 21.84 | 11.81 | 48.82 | 73.37 | 26.48 | Medium |
| **2** | **Almiros** | 8 | 6.61 | 10.51 | 31.22 | 31.21 | 10.92 | 12.52 | 36.72 | 19.96 | Low |
| **3** | **Ag. Ioannis** | 11 | 11.53 | 42.65 | 6.48 | 18.00 | 5.55 | 100 | 16.32 | 28.55 | Medium |
| **4** | **Alfios Delta** | 4 | 13.72 | 29.85 | 43.00 | 4.75 | 27.46 | 42.19 | 38.29 | 28.38 | Medium |
| **5** | **Ag. Petros** | 3 | 13.82 | 26.13 | 35.87 | 36.15 | 70.62 | 100 | 38.04 | 44.95 | High |
| **6** | **Santava** | 5 | 8.71 | 40.00 | 29.59 | 18.94 | 26.93 | 100 | 84.24 | 42.71 | High |
| **7** | **Kinetta** | 11 | 11.73 | 45.46 | 48.53 | 26.75 | 46.77 | 100 | 37.84 | 43.39 | High |
| **8** | **Astros** | 6 | 18.67 | 31.79 | 63.11 | 1.81 | 55.75 | 100 | 55.14 | 46.48 | Very high |
| **9** | **Milopotamos** | 5 | 22.68 | 17.81 | 54.78 | 25.73 | 5.40 | 100 | 83.16 | 42.38 | High |
| **10** | **Marathon** | 8 | 22.25 | 14.75 | 48.99 | 43.77 | 22.63 | 100 | 59.00 | 41.36 | High |
| **11** | **Korission Lagoon** | 10 | 13.66 | 22.81 | 18.74 | 22.33 | 22.63 | 100 | 47.07 | 33.73 | Medium |
| **12** | **Alexandroupolis** | 3 | 11.30 | 17.28 | 48.47 | 25.84 | 9.00 | 100 | 27.43 | 33.57 | Medium |
| **13** | **Vatera** | 11 | 26.75 | 18.95 | 56.82 | 5.07 | 8.36 | 25.07 | 82.98 | 31.64 | Medium |
| **14** | **Ag. Anna** | 9 | 15.08 | 41.62 | 26.92 | 8.73 | 3.43 | 60.51 | 58.69 | 30.09 | Medium |
| **15** | **Skala Katerinis** | 4 | 12.47 | 26.98 | 79.42 | 29.70 | 23.21 | 33.18 | 73.16 | 37.61 | High |
| **16** | **Achivadolimni** | 3 | 23.09 | 18.91 | 20.85 | 44.04 | 6.89 | 100 | 80.94 | 38.96 | High |
| **17** | **Rethymnon** | 15 | 15.82 | 60.32 | 21.28 | 46.46 | 29.31 | 72.10 | 54.58 | 42.59 | High |
| **18** | **Gouves** | 9 | 8.10 | 38.07 | 64.01 | 35.04 | 57.38 | 100 | 100 | 57.18 | Very high |

beach (location 1, figure 3), BVI attains values between 20 and 27, suggesting a rather homogenous behavior involving small rates of erosion, which is in agreement with the findings of a recently published work[53], wherein it is stated that from 2005 to 2012 the shoreline has retreated uniformly only a few meters. Finally, BVI for the Vatera beach (location 13, figure 3) shows high vulnerability values in its central sectors (45.38), compared to both outer parts (30.81 and 27.44), with the former sectors being associated with shoreline retreat in the order of 4–5 m[54], when the latter seems to be rather stable.

## Concluding comments

The advantage of the developed BVI, compared to other similar vulnerability assessment methods applicable to beaches[55], which usually deal with one process (i.e. storm impact[23]) lies upon its holistic approach to the processes controlling beach evolution; the latter can be represented numerically and integrated quantitatively and qualitatively. Moreover, the equal contribution of the seven (7) indicators not only diminishes the subjectivity in weighting index's indicators[50], but also reveals the principal processes through the quantitatively identification of their relevant significance in beach evolution.

The Beach Vulnerability Index could be improved further, in terms of numerical estimations of its indicators, in terms of both data and processing capacity, as it operates independently to index ranking. On the other hand, the index could incorporate more advanced methods (such as numerical models) for more accurate calculation of index variables. But, this will require more data and processing effort, making the Index less functional for non-expert users.

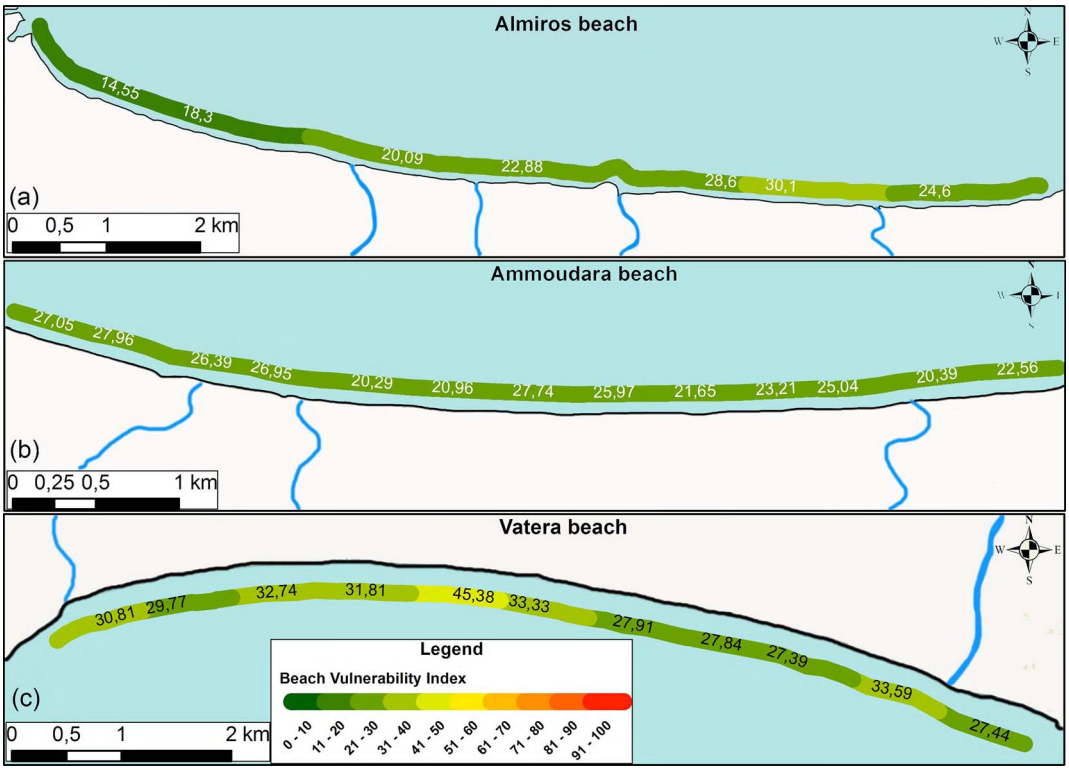


**Figure 4 | Graphical presentation of the results of BVI at Almiros (a), Ammoudara beach (b) and Vatera (c).** Maps were created with ArcMap 9.3.

Finally, this probabilistic evaluation of beach erosion, operating in different physio-geographical settings, we believe that it provides coastal zone managers with additional input towards risk assessment, by prioritizing beaches and/or beach sectors where coastal defences are needed, contributing, therefore, to a more effective response to erosion phenomena and to adaptation to climate change.

## Methods

For the morphological analysis of the test areas topographic maps (1 : 50,000) and diagrams (1 : 5,000), hydrographic charts (1 : 5,000), aerial and satellite images imported in ArcGIS[56] were used. Detailed *in-situ* morphological measurements included 138 shore-normal beach profiles in the centre of the beach sector, extending from the maximum beach elevation to a mean water depth of 15 m. We obtained the sub-aerial and shallow parts of all profiles with a Differential Geographical Positioning System (DGPS), whilst offshore depths were obtained using a small boat equipped with an echo sounder. For the study of the textural characteristics of the coastal sediments, we collected 690 surficial sediment samples from the subaerial and subaqueous parts of the 138 profiles using a cylindrical sediment sampler 5 cm in diameter and 15 cm height. Subsequently, the upper 2–5 cm of each sample were used for the grain size analysis, according to Folk's[57] analytical procedure and using 0.5 $\phi$ sieve intervals. For statistical elaboration and the classification of sediment samples with respect to their grain size and texture, we have also used Folk's[57] formulae. The offshore wave climate (significant height and period) were derived from either local available data sheets (waves and wind) and/or the ERA_INTERIM[58] data base. We estimated nearshore wave characteristics (wave breaking height and angle) using a numerical model established in Matlab.


1. Pranzini, E. & Williams, A. *Coastal erosion and protection in Europe*. 457 (Earthscan, 2013).
2. EUROSION. Living with coastal erosion in Europe: Sediment and Space for Sustainability. PART I - Major findings and Policy Recommendations of the EUROSION project. 57 (Directorate General Environment, European Commission, 2004).
3. Hillyer, T. M. Shoreline Protection and Beach Erosion Control Study. Final Report: An Analysis of the US Army Corps of Engineers Shore Protection Program. (DTIC Document, 1996).
4. Defeo, O., McLachlan, A., Schoeman, D. S., Schlacher, T. A., Dugan, J., Jones, A., Lastra, M. & Scapini, F. Threats to sandy beach ecosystems: A review. *Est. Coast. Shelf Sci.* **81**, 1–12 (2009).
5. Gopalakrishnan, S., Smith, M. D., Slott, J. M. & Murray, A. B. The value of disappearing beaches: A hedonic pricing model with endogenous beach width. *J. Environ. Econ. Manage.* **61**, 297–310 (2011).
6. Houston, J. R. The Economic Value of Beaches: A 2013 Update. *Shore Beach* **81**, 3–11 (2013).
7. Carter, R. W. G. & Woodroffe, C. D. *Coastal Evolution: Late Quaternary Shoreline Morphodynamics*. 540 (Cambridge University Press, 1997).
8. Riggs, S. R. & Ames, D. P. *Effect of Storms on Barrier Island Dynamics, Core Banks, Cape Lookout National Seashore, North Carolina, 1960–2001*. 86 (U.S. Geological Survey, 2007).
9. Berthot, A. & Pattiaratchi, C. Mechanisms for the formation of headland-associated linear sandbanks. *Cont. Shelf Res.* **26**, 987–1004 (2006).
10. Nicholls, R. J., Leatherman, S. P., Dennis, K. C. & Volonté, C. R. Impacts and Responses to Sea-Level Rise: Qualitative and Quantitative Assessments. *J. Coast. Res.* 26–43 (1995).
11. Nicholls, R. J. Impacts of and responses to sea-level rise. in *Understanding sea-level rise and variability* (eds Church, J., Woodworth, P. L., Aarup, T. & Wilson, S., 17–51 (2010).
12. Miselis, J. L. & McNinch, J. E. Calculating shoreline erosion potential using nearshore stratigraphy and sediment volume: Outer Banks, North Carolina. *J. Geophys. Res.- Earth* **111**, F02019 (2006).
13. Cowell, P. J. & Thom, B. G. Morphodynamics of coastal evolution in *Coastal evolution, Late Quaternary shoreline morphodynamics* (eds Carter, R. W. G. & Woodroffe, C. D.) 33–86, (Cambridge University Press, 1995).
14. Kraus, N. C., Larson, M. & Kriebel, D. L. Evaluation of beach erosion and accretion predictors. *Proc. Coastal Sediments '91* (ASCE, New York), 572–587 (1991).
15. Gornitz, V. M., Daniels, R. C., White, T. W. & Birdwell, K. R. The Development of a Coastal Risk Assessment Database: Vulnerability to Sea-Level Rise in the U.S. Southeast. *J. Coast. Res.* 327–338 (1994).
16. Özyurt, G. & Ergin, A. Improving Coastal Vulnerability Assessments to Sea-Level Rise: A New Indicator-Based Methodology for Decision Makers. *J. Coast. Res.* 265–273 (2010).
17. Cooper, N. J. & Jay, H. Predictions of large-scale coastal tendency: development and application of a qualitative behaviour-based methodology. *J. Coast. Res.* **36** (2002).
18. Kumar, T. S., Mahendra, R. S., Nayak, S., Radhakrishnan, K. & Sahu, K. C. Coastal Vulnerability Assessment for Orissa State, East Coast of India. *J. Coast. Res.* 523–534 (2010).
19. Bruun, P. Sea level rise as a cause of shore erosion. *ASCE J. Water Harb Div.* **88**, 117–130 (1962).
20. Dean, R. G. Equilibrium beach profiles: characteristics and applications. *J. Coast. Res.* **7**, 53–84 (1991).
21. Carter, T. R., Parry, M. L., Harasawa, H. & Nishioka, S. *Technical Guidelines for Assessing Climate Change Impacts and Adaptations*. (University College London, Centre for Global Environmental Research, and National Institute for Environmental Studies, 1994).
22. Jimenez, J. *et al.* Geomorphic coastal vulnerability to storms in microtidal fetch-limited environments: application to NW Mediterranean & N Adriatic Seas. *J. Coast. Res.* **SI56**, 1641–1645 (2009).
23. Bosom, E. & Jiménez, J. A. Probabilistic coastal vulnerability assessment to storms at regional scale – application to Catalan beaches (NW Mediterranean). *Nat. Hazards Earth Syst. Sci.* **11**, 475–484 (2011).
24. Sousa, P. H. G. O., Siegle, E. & Tessler, M. G. Vulnerability assessment of Massaguaçú Beach (SE Brazil). *Ocean Coast. Manage.* **77**, 24–30 (2013).
25. Vousdoukas, M. I., Wziatek, D. & Almeida, L. P. Coastal vulnerability assessment based on video wave run-up observations at a meso-tidal, reflective beach. *Ocean Dynam.* **62**, 123–137 (2012).
26. Hinkel, J. *et al.* A global analysis of erosion of sandy beaches and sea-level rise: An application of DIVA. *Global Planet. Change* **111**, 150–158 (2013).
27. Alexandrakis, G., Poulos, S., Petrakis, S. & Collins, M. The development of a Beach Vulnerability Index (BVI) for the assessment of erosion in the case of the North Cretan Coast (Aegean Sea). *Hell. J.Geosc.* **45**, 11–22 (2010).
28. Bernabeu, A. M., Medina, R. & Vidal, C. A morphological model of the beach profile integrating wave and tidal influences. *Mar. Geol.* **197**, 95–116 (2003).
29. Hallermeier, R. J. A profile zonation for seasonal sand beaches from wave climate. *Coast. Eng.* **4**, 253–277 (1980).
30. You, Z.-J. & Yin, B. A unified criterion for initiation of sediment motion and inception of sheet flow under water waves. *Sedimentology* **53**, 1181–1190 (2006).
31. Komar, P. D. *Beach Processes and Sedimentation*. 2nd edn, 429, (Prentice Hall, 1998).
32. Hattori, M. & Kawamata, R. Onshore-offshore transport and beach profile change. *Proc. 17th Coastal Conf., ASCE* **2**, 1175–1193 (New York, 1980).
33. Bailard, J. A. & Inman, D. L. An energetics bedload model for a plane sloping beach: Local transport. *J. Geophys. Res., C.* **86**, 2035–2043 (1981).
34. Bailard, J. A. An cnergetics total load sediment transport model for a plane sloping beach. *J. Geophys. Res.* **86**, 10938–10954 (1981).
35. Hovius, N. Controls on sediment supply by large rivers in *Relative Role of Eustacy, Climate, and Tectonism in Continental Rocks* (eds Shanley, K. W. & McCabe, P. J.) 3–16, (Special Publication, Society of Economic Paleontologists and Mineralogists, 1998).
36. Dendy, F. & Bolton, G. Sediment yield-runoff-drainage area relationships in the United States. *J. Soil Water Conserv.* **31**, 264–266 (1976).
37. Jansen, J. M. & Painter, R. B. Predicting sediment yield from climate and topography. *J. Hydrol.* **21**, 371–380 (1974).
38. Hrissanthou, V. Estimate of sediment yield in a basin without sediment data. *Catena* **64**, 333–347 (2005).
39. Bray, M. J. & Hooke, J. *Prediction of soft-cliff retreat with accelerating sea-level rise*. *J. Coast. Res.* **13**, 453–467 (1997).
40. Walkden, M. J. A. & Hall, J. W. A predictive Mesoscale model of the erosion and profile development of soft rock shores. *Coast. Eng.* **52**, 535–563 (2005).
41. Healy, T. Sea level rise and impacts on nearshore sedimentation: an overview. *Geol Rundsch* **85**, 546–553 (1996).
42. Bruun, P. Coast erosion and the development of beach profiles. *U.S. Army Beach Erosion Board Technical Memorandum No. 44* (1954).
43. Cooper, J. A. G. & Pilkey, O. H. Sea-level rise and shoreline retreat: time to abandon the Bruun Rule. *Global Planet Change* **43**, 157–171 (2004).
44. Velegrakis, A. F. *et al.* Beach erosion prediction for the Black Sea coast, due to sea level rise. in *9th MEDCOAST Conf.* Sochi, Russia **1**, 776–787, (Sochi, Russia, 2009).
45. Stockdon, H. F., Holman, R. A., Howd, P. A. & Sallenger, J. A. H. Empirical parameterization of setup, swash, and runup. *Coast. Eng.* **53**, 573–588 (2006).
46. Vousdoukas, M. I., Velegrakis, A. F., Dimou, K., Zervakis, V. & Conley, D. C. Wave run-up observations in microtidal, sediment-starved pocket beaches of the Eastern Mediterranean. *J Marine Syst.* **78**, S37–S47 (2009).
47. Hsu, S. A. Correction of Land-Based Wind Data for Offshore Applications: A Further Evaluation. *J. Phys. Oceanogr.* **16**, 390–394 (1986).
48. Chapman, D. M. Aeolian sand transport–an optimized model. *Earth Surf. Proc. Land.* **15**, 751–760 (1990).
49. Bagnold, R. A. *The Physics of Blown Sand and Desert Dunes*. 320 (Methuen & Company: William Morrow, 1941).
50. Villa, F. & McLeod, H. Environmental Vulnerability Indicators for Environmental Planning and Decision-Making: Guidelines and Applications. *Environ. Manage.* **29**, 335–348 (2002).
51. Scott, T., Masselink, G. & Russell, P. Morphodynamic characteristics and classification of beaches in England and Wales. *Mar. Geol.* **286**, 1–20 (2011).
52. Petrakis, S., Alexandrakis, G. & Poulos, S. Recent and future trends of beach zone evolution in relation to its physical characteristics: the case of the Almiros bay (island of Crete, South Aegean Sea). *Global Nest J.* **16**, 104–113 (2013).

53. Alexandrakis, G., Ghionis, G. & Poulos, S. The Effect of Beach Rock Formation on the Morphological Evolution of a Beach. The Case Study of an Eastern Mediterranean Beach: Ammoudara, Greece. *J. Coast. Res.* **SI 69**, 47–59 (2013).
54. Vousdoukas, M. I., Velegrakis, A. F. & Karambas, T. V. Morphology and sedimentology of a microtidal beach with beachrocks: Vatera, Lesbos, NE Mediterranean. *Cont. Shelf Res.* **29**, 1937–1947 (2009).
55. Mendoza, E. T. & Jiménez, J. A. Storm-Induced Beach Erosion Potential on the Catalonian Coast. *J. Coast. Res.* 81–88 (2006).
56. ESRI. ArcMap 9.2. Redlands, California patent (2009).
57. Folk, R. L. *Petrology of the Sedimentary Rocks*, 182, (Hemphill Publishing Company, 1980).
58. European Centre for Medium-Range Weather, F. (Research Data Archive at the National Center for Atmospheric Research, Computational and Information Systems Laboratory, Boulder, CO, 2009).

## Acknowledgments

G. Alexandrakis was supported by the Action "Supporting Postdoctoral Researchers" of the Operational Program "Education and Lifelong Learning" (Action's Beneficiary: General Secretariat for Research and Technology), which is co-financed by the European Social Fund (ESF) and the Greek State. The authors would also like to thank Prof. Michael Collins for his constructive comments and his contribution to manuscript editing.

## Author contributions

G.A. developed the model and carried out the analyses as part of his PhD thesis, while S.P. had supervised the thesis that concluded in 2011. Both authors discussed the results and contributed to the preparation of the manuscript.

## Additional information

**Competing financial interests:** The authors declare no competing financial interests.

**How to cite this article:** Alexandrakis, G. & Poulos, S.E. An holistic approach to beach erosion vulnerability assessment. *Sci. Rep.* **4**, 6078; DOI:10.1038/srep06078 (2014).